

# Perspectives on preservation of physical properties through optimization

Pavel Bochev    Denis Ridzal    Kara Peterson  
Sandia National Laboratories

in collaboration with

Mikhail Shashkov (LANL)



High-Resolution Mathematical and Numerical Analysis of Involution-Constrained PDEs  
Oberwolfach, September 15-20, 2013

Sandia National Laboratories is a multi-program laboratory managed and operated by Sandia Corporation, a wholly owned subsidiary of Lockheed Martin Corporation, for the U.S. Department of Energy's National Nuclear Security Administration under contract DE-AC04-94AL85000.

# Inventory of properties - a prequel

## Structural:

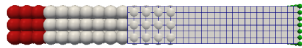
- DeRham cohomology; inf-sup conditions; conservation...
- Typically achieved *by topological means*:
  - careful placement of the variables on the mesh;
  - special grid structure, e.g., topologically dual grids
- **Game changer:** *Discrete exterior calculus, mimetic FD,*
- **Challenges:** PDEs that won't fit neatly in a cohomological structure
  - **Diminishing returns for complex, nonlinear multiphysics problems?**

## Qualitative:

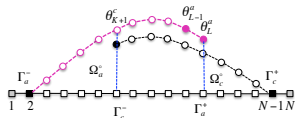
- Maximum principle, local solution bounds, symmetries.
- Correlations between variables: e.g., between two passive tracers.
- **Challenges:** conventional ways to preserve these properties typically
  - impose restrictions on the mesh, .e.g, Cartesian, and/or
  - entangle accuracy with the preservation of the property,
- **Game changer:** *Optimization? May be, but not yet...*

# Optimization strategy - an overview

Atomistic-to-continuum coupling



ATOMISTIC MODEL    FINITE ELEMENTS



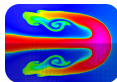
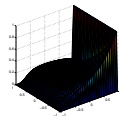
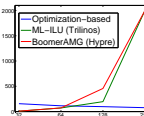
Optimization-based modeling (DOE/ASCR)

$$\min_u \|u - u^T\|$$

$$\text{s.t. } L^h(u) \geq 0$$

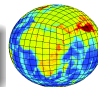
Operator splitting and solver synthesis

Study	Fixed diffusion: $10^{-8}$			Fixed grid size: 128		
	64	128	256	$10^{-2}$	$10^{-4}$	$10^{-6}$
OBM-ML <sup>SGS</sup>	114	97	77	62	97	97
ML <sup>LU</sup>	71	196	—	9	96	196
BAMG	72	457	—	7	33	457



ALE

Feature-preserving solution transfer



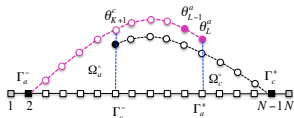
SEMI-LAGRANGIAN

# Optimization strategy - an overview

Atomistic-to-continuum  
coupling



ATOMISTIC MODEL    FINITE ELEMENTS



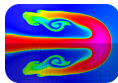
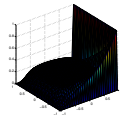
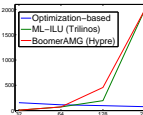
Operator splitting and  
solver synthesis

Study	Fixed diffusion: $10^{-8}$			Fixed grid size: 128		
	64	128	256	$10^{-2}$	$10^{-4}$	$10^{-6}$
OBM-ML <sup>SGS</sup>	114	97	77	62	97	97
ML <sup>LU</sup>	71	196	—	9	96	196
BAMG	72	457	—	7	33	457

Optimization-based modeling  
(DOE/ASCR)

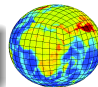
$$\min_u \|u - u^T\|$$

$$\text{s.t. } L^h(u) \geq 0$$



ALE

Feature-preserving  
solution transfer



SEMI-LAGRANGIAN

## Solution transfer

## Scalar mass-density remap

## Flux form of optimization-based remap

- Mathematical formulation

- Theoretical properties and benefits

- Algorithm and computational cost

## Mass form of optimization-based remap

- Mathematical formulation

- Algorithm and computational cost

## Flexibility of OBR

- Optimization-based transport on the sphere

- Adaptable targets and smoothness indicators

- Passive tracer transport

- High-order remap: BLAST, HOMME

- Tensor remap: ALEGRA

## Solution transfer

### Scalar mass-density remap

### Flux form of optimization-based remap

Mathematical formulation

Theoretical properties and benefits

Algorithm and computational cost

### Mass form of optimization-based remap

Mathematical formulation

Algorithm and computational cost

### Flexibility of OBR

Optimization-based transport on the sphere

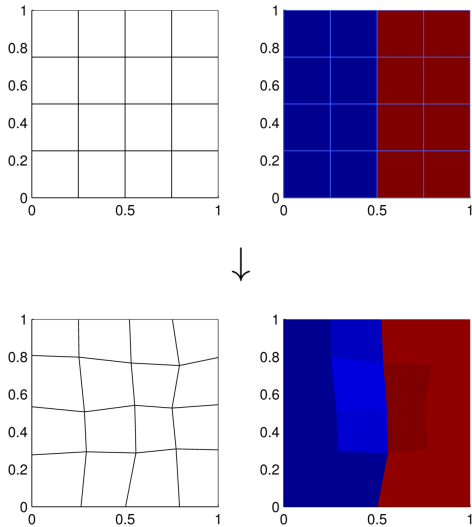
Adaptable targets and smoothness indicators

Passive tracer transport

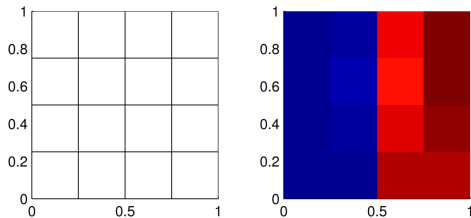
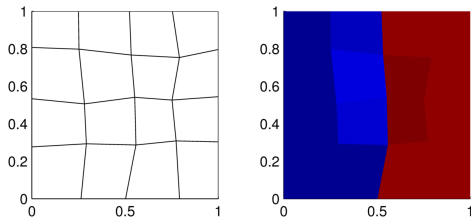
High-order remap: BLAST, HOMME

Tensor remap: ALEGRA

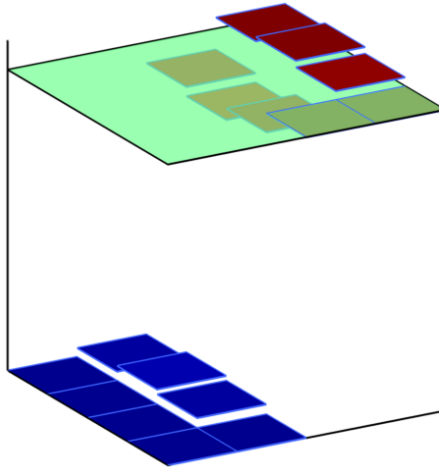
# Solution transfer



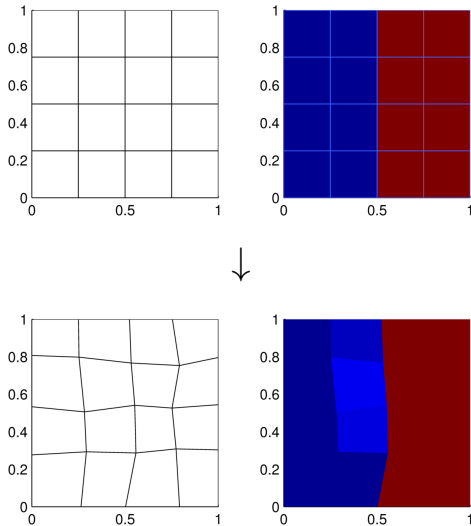
# Solution transfer



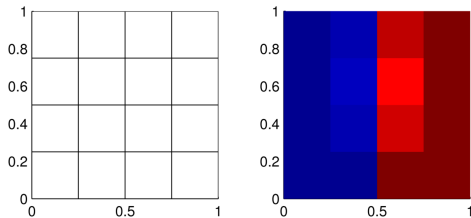
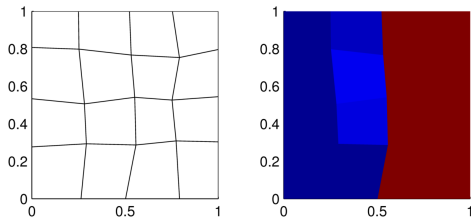
# Solution transfer



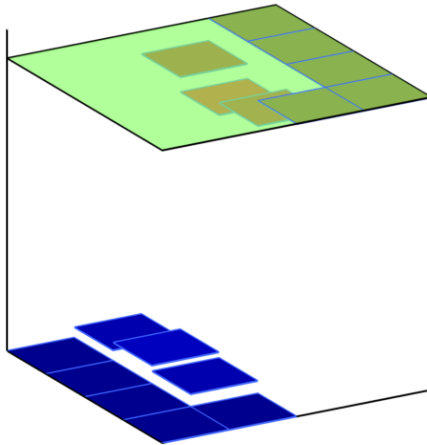
# Solution transfer



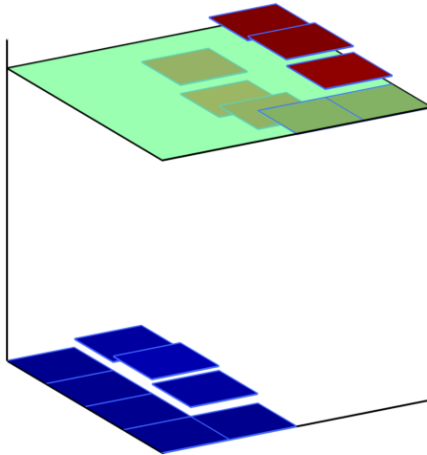
# Solution transfer



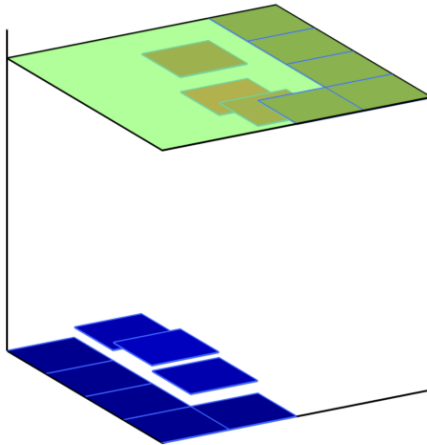
# Solution transfer



# Solution transfer



# Solution transfer



# Solution transfer

**Given:** Discrete representation  $\mathbf{f}_A$  of function  $\mathbf{f}$  on mesh  $\mathbf{A}$ .

**Find:** *Accurate* discrete representation  $\mathbf{f}_B$  of  $\mathbf{f}$  on mesh  $\mathbf{B}$ , subject to physical constraints:

- conservation of mass, energy, etc.
- preservation of monotonicity
- physically meaningful ranges for variables:  
density  $\geq 0$ , concentration  $\in [0, 1]$

## Critical task in computational science:

- shock-hydrodynamics: ALEGRA, BLAST, etc.
- tracer transport: sea ice – CICE, atmosphere – HOMME, etc.
- mesh repair, rezone, untangling, reconnection, conservative regridding in, e.g., big ocean data
- transfer of simulation data between heterogeneous numerical models
- data visualization on arbitrary polygonal grids
- solution recovery for resilient computing

## Solution transfer

## Scalar mass-density remap

## Flux form of optimization-based remap

Mathematical formulation

Theoretical properties and benefits

Algorithm and computational cost

## Mass form of optimization-based remap

Mathematical formulation

Algorithm and computational cost

## Flexibility of OBR

Optimization-based transport on the sphere

Adaptable targets and smoothness indicators

Passive tracer transport

High-order remap: BLAST, HOMME

Tensor remap: ALEGRA

## Mass-density remap

**Given:** Old mesh  $C(\Omega)$  and mean density values  $\rho_i$  on old mesh cells  $c_i$ .

**Find:** Approximations  $\tilde{m}_i$  of masses on a new mesh  $\tilde{C}(\Omega)$  with cells  $\tilde{c}_i$ ,

$$\tilde{m}_i \approx \tilde{m}_i^{\text{exact}} = \int_{\tilde{c}_i} \rho(\mathbf{x}) dV, \quad i = 1, \dots, C; \quad \text{subject to}$$

**C1. Mass conservation:**  $\sum_{i=1}^C \tilde{m}_i = \sum_{i=1}^C m_i = M$ .

**C2. Second-order accuracy:** If  $\rho(\mathbf{x})$  is a global linear function on  $\Omega$ , then the mass approximations are exact,

$$\tilde{m}_i = \tilde{m}_i^{\text{exact}} = \int_{\tilde{c}_i} \rho(\mathbf{x}) dV, \quad i = 1, \dots, C.$$

**C3. Local bounds:** The approximations of the mean density on the new cells,  $\tilde{\rho}_i = \tilde{m}_i / V(\tilde{c}_i)$ , are bounded by the old neighborhood extrema

$$\rho_i^{\min} \leq \tilde{\rho}_i \leq \rho_i^{\max}, \quad i = 1, \dots, C, \quad \text{or equivalently,}$$

$$\tilde{m}_i^{\min} := \rho_i^{\min} V(\tilde{c}_i) \leq \tilde{m}_i \leq \rho_i^{\max} V(\tilde{c}_i) =: \tilde{m}_i^{\max}, \quad i = 1, \dots, C.$$

# Some history

## 19xx–2010:

- Scalar remap is a long-studied problem.
- The constraints (C1)–(C3) are typically handled *by construction*:
  - a careful choice of variables in the remap scheme;
  - a special reconstruction procedure; and
  - a particular choice of ‘limiter’ (WIKIPEDIA: 15 slope limiters).
- Challenges: accuracy loss, mesh/cell dependence, robustness.
- **Game changer:**  
*Flux-corrected remap (FCR), Shashkov et al., J. Comp. Phys., 2010.*

## 2010–2012:

- We use globally constrained optimization to reconcile (C1)–(C3).
- A mathematically rigorous way to handle constraints.
- Elegant theory, and connections to methods like FCR.
- Improved accuracy; improved robustness; general applicability.

## 2012–2013:

- Optimization-based remap at the cost of conventional remap.

## Solution transfer

## Scalar mass-density remap

## Flux form of optimization-based remap

Mathematical formulation

Theoretical properties and benefits

Algorithm and computational cost

## Mass form of optimization-based remap

Mathematical formulation

Algorithm and computational cost

## Flexibility of OBR

Optimization-based transport on the sphere

Adaptable targets and smoothness indicators

Passive tracer transport

High-order remap: BLAST, HOMME

Tensor remap: ALEGRA

# Flux form of OBR

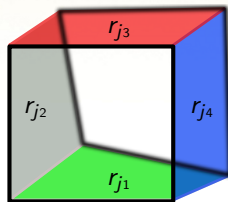
1. Given the side-to-cell incidence matrix  $\mathbf{D}$ , or *discrete divergence*, define **mass update**

$$\tilde{m} = m + \mathbf{D}F,$$

where  $F$  approximates the exact **fluxes** over the swept regions  $r_j$ ,

$$F_j \approx F_j^{\text{exact}} = \int_{r_j} \rho(\mathbf{x}) dV; \quad j = 1, \dots, S.$$

2. Compute **target**  $F_j^T := \int_{r_j} \rho^h(\mathbf{x}) dV$ ,  $j = 1, \dots, S$ , for some density reconstruction  $\rho^h(\mathbf{x})$  that is **exact for linear functions**. Solve:



$$\begin{aligned} \tilde{m}_i &= m_i + (\mathbf{D}F)_i = \\ & m_i + \sum_{k \in \{j1, \dots, j4\}} \sigma_k F_k \end{aligned}$$

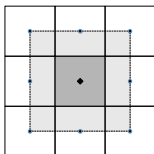
$$\begin{cases} \text{minimize}_F & \frac{1}{2} \|F - F^T\|_{\ell_2}^2 & \text{subject to} \\ \tilde{m}^{\min} & \leq m + \mathbf{D}F \leq \tilde{m}^{\max}. \end{cases}$$

# Immediate properties

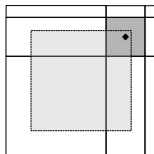
- Local bounds are enforced directly:  $\tilde{m}^{\min} \leq m + \mathbf{DF} \leq \tilde{m}^{\max}$ .
- Mass conservation is implicit: follows from the divergence form

$$\sum_{i=1}^C \tilde{m}_i = \sum_{i=1}^C m_i + \underbrace{\sum_{i=1}^C (\mathbf{DF})_i}_{=0, \text{ divergence form}} = \sum_{i=1}^C m_i.$$

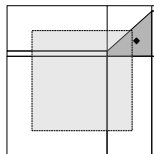
- Theorem: Second-order accuracy.** A sufficient condition for OBR to recover linear densities **exactly** is that the centroid of any new cell remain in the **convex hull** of the centroids of its old neighbors.



(a) original



(b) admissible



(c) inadmissible

Less restrictive!

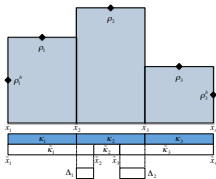
- Independent of dimension and cell topology.
- Separation of concerns: Optimally accurate and monotone!

# Relation to Flux-Corrected Remap (FCR)

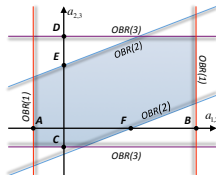
**Theorem.** FCR can be formulated as a **global optimization problem**.

- (1) The FCR cost function is equivalent to the OBR cost function.
- (2) The FCR feasible set is **always a subset** of the OBR feasible set.

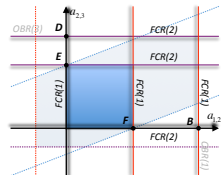
Compressive Mesh Motion



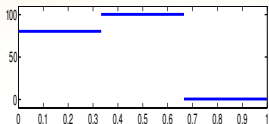
OBR Feasible Set



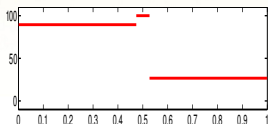
FCR Feasible Set



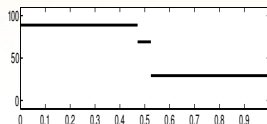
# 1. OBR preserves shape when FCR may not



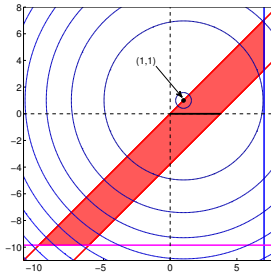
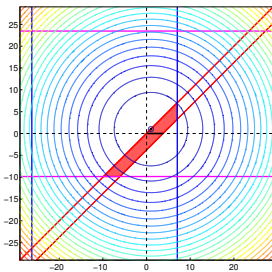
Original



After a single OBR step



After a single FCR step



Level sets of the cost function and the feasible sets:

**Red region** = OBR feasible set; contains flux target  $F^T = (1,1)$ .

**Solid horizontal segment (black)** = FCR feasible set.

## 2. OBR preserves monotonicity when FCR may not

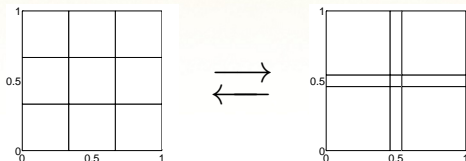


**Figure:** A  $3 \times 3$  uniform initial grid (left pane) and the compressed “torture” grid (right pane) with a  $4 \times 4$ -fold compression of the middle cell.

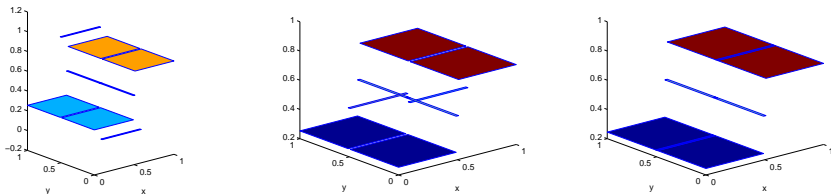
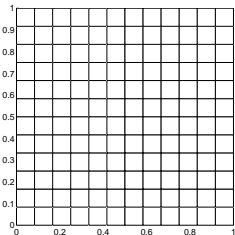
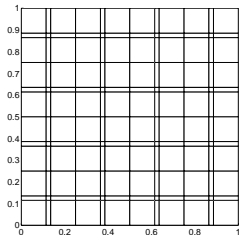


**Figure:** Linear density  $\rho(x, y) = x$  remapped from the uniform  $3 \times 3$  grid to the compressed “torture” grid with  $\ell = 16$ . Left to right: the donor-cell method, FCR, OBR. It is clear that OBR gives the best density approximation.

# 3. OBR is more accurate than FCR



Remap of smooth (sine) density using OBR

#cells	#remaps	$L_1$ err	$L_2$ err	$L_\infty$ err	$L_1$ rate	$L_2$ rate	$L_\infty$ rate
128×128	640	2.69e-04	3.65e-04	2.03e-03	—	—	—
256×256	1280	6.71e-05	9.08e-05	5.07e-04	<b>2.00</b>	<b>2.01</b>	<b>2.00</b>
512×512	2560	1.68e-05	2.27e-05	1.20e-04	<b>2.00</b>	<b>2.00</b>	<b>2.04</b>
1024×1024	5120	4.19e-06	5.66e-06	2.69e-05	<b>2.00</b>	<b>2.00</b>	<b>2.08</b>

Remap of smooth (sine) density using FCR

#cells	#remaps	$L_1$ err	$L_2$ err	$L_\infty$ err	$L_1$ rate	$L_2$ rate	$L_\infty$ rate
128×128	640	2.81e-04	3.47e-04	1.23e-03	—	—	—
256×256	1280	9.23e-05	1.19e-04	5.14e-04	1.61	1.54	1.26
512×512	2560	3.65e-05	5.05e-05	2.50e-04	1.47	1.39	1.15
1024×1024	5120	1.69e-05	2.39e-05	1.24e-04	1.35	1.28	1.10

# Flux-form OBR algorithm

## How about speed?

Rather than solve

$$\left\{ \begin{array}{l} \underset{F}{\text{minimize}} \quad \frac{1}{2} \|F - F^T\|_{\ell_2}^2 \quad \text{subject to} \\ \tilde{m}^{\min} - m \leq \mathbf{D}F \leq \tilde{m}^{\max} - m \end{array} \right.$$

directly, we solve its equivalent **dual reformulation**

$$\left\{ \begin{array}{l} \underset{\lambda, \mu}{\text{minimize}} \quad \frac{1}{2} \|\mathbf{D}^T \lambda - \mathbf{D}^T \mu\|_2^2 - \langle \lambda, \tilde{m}^{\min} - m - \mathbf{D}F^T \rangle \\ \quad \quad \quad - \langle \mu, -\tilde{m}^{\max} + m + \mathbf{D}F^T \rangle \\ \text{subject to} \quad \lambda \geq 0, \mu \geq 0. \end{array} \right.$$

Thus, we trade the complexity in the globally coupled inequality constraint for a more complex objective function.

# Flux-form OBR algorithm

## Some notation

- Define system matrix  $\mathbf{H} \in \mathbb{R}^{2C \times 2C}$  and vector  $b \in \mathbb{R}^{2C}$

$$\mathbf{H} = \begin{bmatrix} \mathbf{D}\mathbf{D}^T & -\mathbf{D}\mathbf{D}^T \\ -\mathbf{D}\mathbf{D}^T & \mathbf{D}\mathbf{D}^T \end{bmatrix} \quad b = \begin{bmatrix} \mathbf{D}\mathbf{F}^T - \tilde{m}^{\min} + m \\ -\mathbf{D}\mathbf{F}^T + \tilde{m}^{\max} - m \end{bmatrix}$$

- Define the diagonal operator,  $\text{Diag} : \mathbb{R}^{2C} \rightarrow \mathbb{R}^{2C \times 2C}$ , as

$$[\text{Diag}(x)]_{ij} = \begin{cases} x_i & \text{when } i = j \\ 0 & \text{" } i \neq j \end{cases} .$$

- Define the operator  $v : \mathbb{R}^{2C} \rightarrow \mathbb{R}^{2C}$  as

$$[v(x)]_i = \begin{cases} x_i & \text{when } [\mathbf{H}x + b]_i \geq 0 \\ 1 & \text{" } [\mathbf{H}x + b]_i < 0 \end{cases} .$$

- Define the operator  $K : \mathbb{R}^{2C} \rightarrow \mathbb{R}^{2C \times 2C}$  as

$$[K]_{ii} = \begin{cases} 1 & \text{when } [\mathbf{H}x + b]_i \geq 0 \\ 0 & \text{" } [\mathbf{H}x + b]_i < 0 \end{cases} .$$

# Flux-form OBR algorithm

## Semismooth Newton

- It can be shown that under mild assumptions the solution of the bound-constrained problem is equivalent to the solution of the **piecewise differentiable system of equations**

$$\text{Diag}(v(x)) (\mathbf{H}x + b) = 0.$$

- Apply Newton's method to the nonlinear system by solving

$$(K(x)\text{Diag}(\mathbf{H}x + b) + \text{Diag}(v(x)) \mathbf{H}) p = -\text{Diag}(v(x)) (\mathbf{H}x + b)$$

for the update  $p$  at a given iterate  $x$ , followed by  $x \leftarrow x + p$ .

- Each iteration entails the solution of a large linear system.**
- Linear complexity,  $\mathcal{O}(C)$ , where  $C$  is the number of mesh cells.**
- Conjecture: Parallelizes as well as multigrid  $\rightarrow$   $DD^T$  operator.**

**We will examine the speed of this approach in the context of a transport application.**

# Optimization-Based Transport

*We can extend the flux-form OBR to a conservative and bounds preserving scheme (OBT) for the scalar transport equation:*

$$\frac{\partial \rho}{\partial t} + \nabla \cdot \rho \mathbf{v} = 0 \quad \text{on} \quad \Omega \times [0, T], \quad \rho(\mathbf{x}, 0) = \rho_0(\mathbf{x})$$

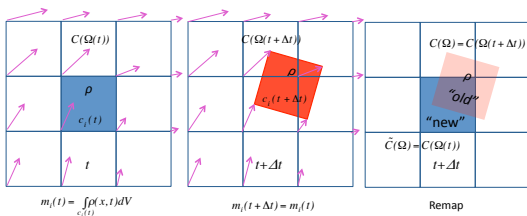
# Optimization-Based Transport

We can extend the flux-form OBR to a conservative and bounds preserving scheme (OBT) for the scalar transport equation:

$$\frac{\partial \rho}{\partial t} + \nabla \cdot \rho \mathbf{v} = 0 \quad \text{on} \quad \Omega \times [0, T], \quad \rho(\mathbf{x}, 0) = \rho_0(\mathbf{x})$$

Incremental remap algorithm (semi-Lagrangian scheme)

- 1 Project departure grid to arrival grid:  $C(\Omega(t)) \mapsto C(\Omega(t + \Delta t))$
- 2 Lagrangian transport:  $m_i(t + \Delta t) = m_i(t)$ ,  $\rho_i(t + \Delta t) = m_i(t) / \mu_i(t + \Delta t)$
- 3 Remap:  $m(t + \Delta t) \mapsto \tilde{m}$  and  $\rho(t + \Delta t) \mapsto \tilde{\rho}$



- cell mass  $m_i = \int_{c_i} \rho(\mathbf{x}, t) dV$
- cell area  $\mu_i = \int_{c_i} dV$
- cell mean density  $\rho_i = m_i / \mu_i$

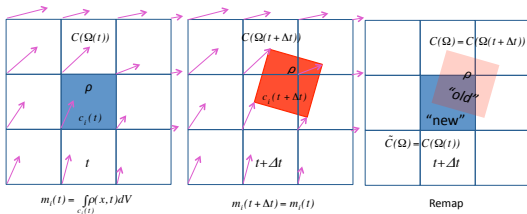
# Optimization-Based Transport

We can extend the flux-form OBR to a conservative and bounds preserving scheme (OBT) for the scalar transport equation:

$$\frac{\partial \rho}{\partial t} + \nabla \cdot \rho \mathbf{v} = 0 \quad \text{on} \quad \Omega \times [0, T], \quad \rho(\mathbf{x}, 0) = \rho_0(\mathbf{x})$$

Incremental remap algorithm (semi-Lagrangian scheme)

- 1 Project departure grid to arrival grid:  $C(\Omega(t)) \mapsto C(\Omega(t + \Delta t))$
- 2 Lagrangian transport:  $m_i(t + \Delta t) = m_i(t)$ ,  $\rho_i(t + \Delta t) = m_i(t) / \mu_i(t + \Delta t)$
- 3 Remap:  $m(t + \Delta t) \mapsto \tilde{m}$  and  $\rho(t + \Delta t) \mapsto \tilde{\rho}$



- cell mass  $m_i = \int_{c_i} \rho(\mathbf{x}, t) dV$
- cell area  $\mu_i = \int_{c_i} dV$
- cell mean density  $\rho_i = m_i / \mu_i$

**OBT inherits the robustness & accuracy of OBR but is it fast?**

# Performance of the flux-form OBTR

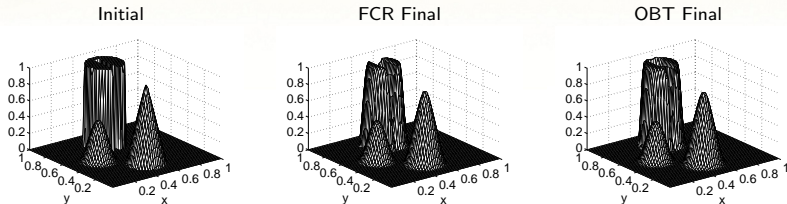


**Figure:** After one full revolution (810 time steps) on a  $128 \times 128$  mesh.

mesh	steps	FCR time(sec)	Flux-OBTR time(sec)	ratio
$64 \times 64$	408	3.3	63.7	19.3
$128 \times 128$	810	26.4	496.4	18.8
$256 \times 256$	1614	229.1	3464.2	15.1

**Table:** Computational cost. **Flux-form OBTR is not competitive!**

## Solution transfer

## Scalar mass-density remap

## Flux form of optimization-based remap

Mathematical formulation

Theoretical properties and benefits

Algorithm and computational cost

## Mass form of optimization-based remap

Mathematical formulation

Algorithm and computational cost

## Flexibility of OBR

Optimization-based transport on the sphere

Adaptable targets and smoothness indicators

Passive tracer transport

High-order remap: BLAST, HOMME

Tensor remap: ALEGRA

# Mass form of OBR

## 1. Define **mass update**

$$\tilde{m} = m + \delta m,$$

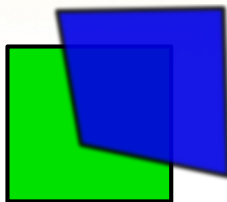
where  $\delta m$  approximates the exact **mass increments** between new and old cells:

$$\delta m_i \approx \delta m_i^{\text{exact}} = \int_{\tilde{c}_i} \rho(\mathbf{x}) dV - \int_{c_i} \rho(\mathbf{x}) dV;$$

where  $i = 1, \dots, C$ .

2. Compute **target**  $\delta m_i^T := \int_{\tilde{c}_i} \rho^h(\mathbf{x}) dV - \int_{c_i} \rho^h(\mathbf{x}) dV$ ,  $i = 1, \dots, C$ , for density  $\rho^h(\mathbf{x})$  that is **exact for linear functions**. Solve:

$$\left\{ \begin{array}{l} \underset{\delta m}{\text{minimize}} \quad \frac{1}{2} \|\delta m - \delta m^T\|_{\ell_2}^2 \quad \text{subject to} \\ \sum_{i=1}^C \delta m_i = 0 \quad \text{and} \quad \tilde{m}^{\min} \leq m + \delta m \leq \tilde{m}^{\max}. \end{array} \right.$$



$$\tilde{m}_i = m_i + \delta m_i$$

Note:  $\delta m_i = (DF)_i$

# Mass-form OBR algorithm

We solve

$$\left\{ \begin{array}{l} \underset{\delta m}{\text{minimize}} \quad \frac{1}{2} \|\delta m - \delta m^T\|_{\ell_2}^2 \quad \text{subject to} \\ \sum_{i=1}^C \delta m_i = 0 \quad \text{and} \quad \tilde{m}^{\min} \leq m + \delta m \leq \tilde{m}^{\max}. \end{array} \right.$$

Known as the **singly linearly constrained QP with simple bounds**, see Dai, Fletcher (2006, Math. Program.).

**Key observation:** The related optimization problem without the mass conservation constraint,  $\sum_{i=1}^C \delta m_i = 0$ , is **fully separable!**

The related problem can be solved by independently (and concurrently) solving  $C$  **one-dimensional** quadratic programs with simple bounds.

**Goal:** Satisfy the second constraint,  $\sum_{i=1}^C \delta m_i = 0$ , “in a few iterations”.

# Mass-form OBR algorithm

We solve

$$\left\{ \begin{array}{l} \underset{\delta m}{\text{minimize}} \quad \frac{1}{2} \|\delta m - \delta m^T\|_{\ell_2}^2 \quad \text{subject to} \\ \sum_{i=1}^C \delta m_i = 0 \quad \text{and} \quad \tilde{m}^{\min} \leq m + \delta m \leq \tilde{m}^{\max}. \end{array} \right.$$

Known as the **singly linearly constrained QP with simple bounds**, see Dai, Fletcher (2006, Math. Program.).

**Key observation:** The related optimization problem without the mass conservation constraint,  $\sum_{i=1}^C \delta m_i = 0$ , is **fully separable!**

The related problem can be solved by independently (and concurrently) solving  $C$  **one-dimensional** quadratic programs with simple bounds.

**Goal:** Satisfy the second constraint,  $\sum_{i=1}^C \delta m_i = 0$ , “in a few iterations”.

# Mass-form OBR algorithm

We solve

$$\left\{ \begin{array}{l} \underset{\delta m}{\text{minimize}} \quad \frac{1}{2} \|\delta m - \delta m^T\|_{\ell_2}^2 \quad \text{subject to} \\ \sum_{i=1}^C \delta m_i = 0 \quad \text{and} \quad \tilde{m}^{\min} \leq m + \delta m \leq \tilde{m}^{\max}. \end{array} \right.$$

Known as the **singly linearly constrained QP with simple bounds**, see Dai, Fletcher (2006, Math. Program.).

**Key observation:** The related optimization problem without the mass conservation constraint,  $\sum_{i=1}^C \delta m_i = 0$ , is **fully separable!**

The related problem can be solved by independently (and concurrently) solving  $C$  **one-dimensional** quadratic programs with simple bounds.

**Goal:** Satisfy the second constraint,  $\sum_{i=1}^C \delta m_i = 0$ , “in a few iterations”.

# Mass-form OBR algorithm

Define Lagrangian functional  $\mathcal{L} : \mathbb{R}^C \times \mathbb{R} \times \mathbb{R}^C \times \mathbb{R}^C \rightarrow \mathbb{R}$ ,

$$\mathcal{L}(\delta m, \lambda, \mu_1, \mu_2) = \frac{1}{2} \sum_{i=1}^C (\delta m_i - \delta m_i^T)^2 - \lambda \sum_{i=1}^C \delta m_i - \sum_{i=1}^C \mu_{1,i} (\delta m_i - \tilde{m}_i^{\min} + m_i) - \sum_{i=1}^C \mu_{2,i} (\tilde{m}_i^{\max} - m_i - \delta m_i),$$

where  $\delta m \in \mathbb{R}^C$  are the primal optimization variables, and  $\lambda \in \mathbb{R}$ ,  $\mu_1 \in \mathbb{R}^C$ , and  $\mu_2 \in \mathbb{R}^C$  are the dual optimization variables.

## KKT conditions:

$$\delta m_i = \delta m_i^T + \lambda + \mu_{1,i} - \mu_{2,i}; \quad i = 1, \dots, C$$

$$\tilde{m}_i^{\min} - m_i \leq \delta m_i \leq \tilde{m}_i^{\max} - m_i; \quad i = 1, \dots, C$$

$$\mu_{1,i} \geq 0, \quad \mu_{2,i} \geq 0; \quad i = 1, \dots, C$$

$$\mu_{1,i} (\delta m_i - \tilde{m}_i^{\min} + m_i) = 0, \quad \mu_{2,i} (-\delta m_i + \tilde{m}_i^{\max} - m_i) = 0; \quad i = 1, \dots, C$$

$$\sum_{i=1}^C \delta m_i = 0$$

# Mass-form OBR algorithm

We solve the KKT conditions directly.

**First**, we focus on the conditions in black, separable in the index  $i$ . For any *fixed* value of  $\lambda$  a solution to the “black” conditions is given by

$$\left\{ \begin{array}{lll} \delta m_i = \delta m_i^T + \lambda; & \mu_{1,i} = \mu_{2,i} = 0 & \text{if } \tilde{m}_i^{\min} - m_i \leq \delta m_i^T + \lambda \leq \tilde{m}_i^{\max} - m_i \\ \delta m_i = \tilde{m}_i^{\min} - m_i; & \mu_{2,i} = 0, \mu_{1,i} = \delta m_i - \delta m_i^T - \lambda & \text{if } \delta m_i^T + \lambda < \tilde{m}_i^{\min} - m_i \\ \delta m_i = \tilde{m}_i^{\max} - m_i; & \mu_{1,i} = 0, \mu_{2,i} = \delta m_i^T - \delta m_i + \lambda & \text{if } \delta m_i^T + \lambda > \tilde{m}_i^{\max} - m_i, \end{array} \right.$$

for all  $i = 1, \dots, C$ .

Ignoring  $\mu_1$  and  $\mu_2$  and treating  $\delta m_i$  as a function of  $\lambda$  yields

$$\delta m_i(\lambda) = \text{median}(\tilde{m}_i^{\min} - m_i, \delta m_i^T + \lambda, \tilde{m}_i^{\max} - m_i), \quad i = 1, \dots, C.$$

This is a trivial, communication-free  $\mathcal{O}(C)$  computation.

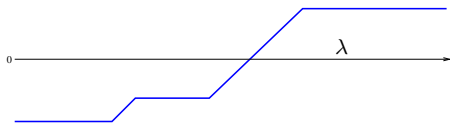
# Mass-form OB algorithm

**Second**, we adjust  $\lambda$  in an outer iteration in order to satisfy

$$\sum_{i=1}^C \delta m_i(\lambda) = 0.$$

When we find the  $\lambda^*$  such that  $\sum_{i=1}^C \delta m_i(\lambda^*) = 0$  holds, we will have solved the full KKT conditions.

The function  $\sum_{i=1}^C \delta m_i(\lambda)$  is a piecewise linear, monotonically increasing function of a single scalar variable  $\lambda$ . Therefore, a **secant method** can be efficiently employed as the outer iteration.



... given  $\lambda_p, \lambda_c, r_p$

① Compute  $\delta m_i(\lambda_c) \leftarrow$   
 $\text{median}(\tilde{m}_i^{\min} - m_i, \delta m_i^T + \lambda_c, \tilde{m}_i^{\max} - m_i) \forall i.$

Compute residual  $r_c \leftarrow \sum_{i=1}^C \delta m_i(\lambda_c).$

② Set  $\alpha \leftarrow (\lambda_p - \lambda_c)/(r_p - r_c)$ . Set  $r_p \leftarrow r_c.$

③ Set  $\lambda_p \leftarrow \lambda_c$ . Set  $\lambda_c \leftarrow \lambda_c - \alpha r_c.$

**In all our examples, the algorithm requires  $\leq 5$  secant iterations!**

# Performance of the mass-form OBT

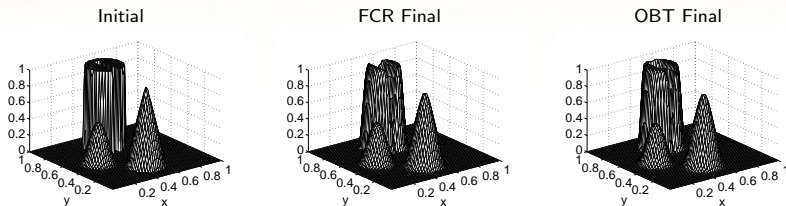


**Figure:** After one full revolution (810 time steps) on a  $128 \times 128$  mesh.

mesh	steps	FCR time(sec)	Flux-OBT time(sec)	ratio	Mass-OBT time(sec)	ratio
$64 \times 64$	408	3.3	63.7	19.3	3.4	1.0
$128 \times 128$	810	26.4	496.4	18.8	26.2	1.0
$256 \times 256$	1614	229.1	3464.2	15.1	222.7	1.0

**Table:** Computational cost. **Mass-form OBT: as fast as an explicit scheme!**

## Solution transfer

## Scalar mass-density remap

## Flux form of optimization-based remap

Mathematical formulation

Theoretical properties and benefits

Algorithm and computational cost

## Mass form of optimization-based remap

Mathematical formulation

Algorithm and computational cost

## Flexibility of OBR

Optimization-based transport on the sphere

Adaptable targets and smoothness indicators

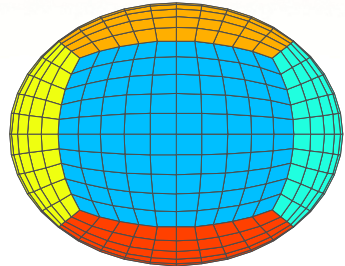
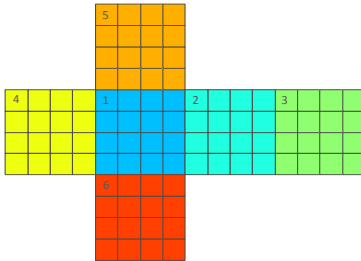
Passive tracer transport

High-order remap: BLAST, HOMME

Tensor remap: ALEGRA

# Optimization-Based Transport on the Sphere

## Adaptation to Cubed Sphere Grid



- Six faces of cube projected onto surface of sphere
- Discontinuous at panel edges
- Avoids polar singularities of lat/lon grid
- OBR/OBT extension boils down to swapping the reconstruction method
- Impervious to cell-shapes: can be applied to arbitrary grids, including polygons.

## Adaptable targets

- Cost-function targets are built from the reconstruction:

$$\rho^h(\mathbf{x})|_{c_i} := \rho_i^h(\mathbf{x}) = \rho_i + \mathbf{g}_i \cdot (\mathbf{x} - \mathbf{b}_i) \quad \forall c_i \in C(\Omega),$$

where  $\rho_i$  are density values on the old cells  $c_i$ ,  $\mathbf{g}_i$  is a least-squares approximation of the gradient  $\nabla \rho$  based on  $\rho_i$  from the cells in the neighborhood  $N(c_i)$ , and  $\mathbf{b}_i$  is the barycenter of  $c_i$ .

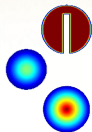
- Define **reconstruction residual**:  $q_i = \sum_{j \in N(c_i)} |\rho_j - \rho_i^h(\mathbf{b}_j)|$ .
- Modify the gradient of  $\rho^h(\mathbf{x})$  to obtain **adaptable reconstruction**:

$$\rho^A(\mathbf{x})|_{c_i} := \rho_i^A(\mathbf{x}) = \rho_i + \alpha_i(q_i) \mathbf{g}_i \cdot (\mathbf{x} - \mathbf{b}_i) \quad \forall c_i \in C(\Omega).$$

- For a given constant  $\gamma > 0$ ,

$$\alpha_i(q_i) = \begin{cases} 1 & \text{if "smooth"} \\ 1 + \gamma q_i / \max_{i=1, \dots, C} \{q_i\} & \text{otherwise.} \end{cases}$$

# Dual variables as smoothness indicators



$$\left\{ \begin{array}{ll} \mu_{1,i} = \mu_{2,i} = 0 & \text{if } \tilde{m}_i^{\min} - m_i \leq \delta m_i^T + \lambda \leq \tilde{m}_i^{\max} - m_i \\ \mu_{2,i} = 0, \mu_{1,i} = (\tilde{m}_i^{\min} - m_i) - \delta m_i^T - \lambda & \text{if } \delta m_i^T + \lambda < \tilde{m}_i^{\min} - m_i \\ \mu_{1,i} = 0, \mu_{2,i} = \delta m_i^T - (\tilde{m}_i^{\max} - m_i) + \lambda & \text{if } \delta m_i^T + \lambda > \tilde{m}_i^{\max} - m_i, \end{array} \right.$$

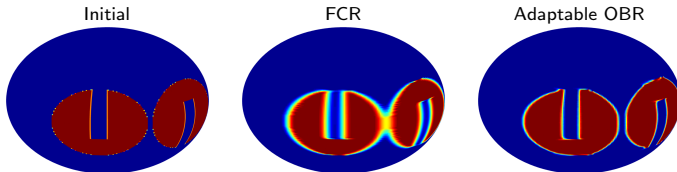


**Figure:** Transport results for the solid-body rotation test on the sphere, for two revolutions, left to right and back (1920 time steps) on a  $0.75^\circ$  mesh.

mesh	steps	FCR time(sec)	Mass-OBR time(sec)	ratio	FCR $L_1$ error	rate	Mass-OBR $L_1$ error	rate
$3^\circ$	480	17.4	18.2	1.0	3.25e-2	—	2.79e-2	—
$1.5^\circ$	960	132.5	151.6	1.1	1.99e-2	0.78	1.36e-3	1.04
$0.75^\circ$	1920	1184.5	1379.0	1.2	1.10e-2	0.78	5.41e-3	1.18

# Dual variables as smoothness indicators

$$\begin{cases} \mu_{1,i} = \mu_{2,i} = 0 & \text{if } \tilde{m}_i^{\min} - m_i \leq \delta m_i^T + \lambda \leq \tilde{m}_i^{\max} - m_i \\ \mu_{2,i} = 0, \mu_{1,i} = (\tilde{m}_i^{\min} - m_i) - \delta m_i^T - \lambda & \text{if } \delta m_i^T + \lambda < \tilde{m}_i^{\min} - m_i \\ \mu_{1,i} = 0, \mu_{2,i} = \delta m_i^T - (\tilde{m}_i^{\max} - m_i) + \lambda & \text{if } \delta m_i^T + \lambda > \tilde{m}_i^{\max} - m_i, \end{cases}$$

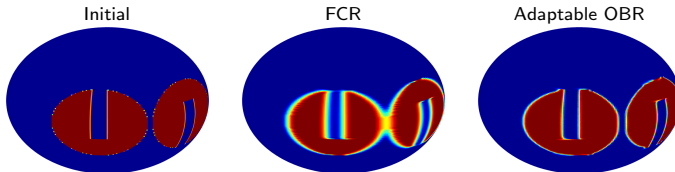


**Figure:** Transport results for the solid-body rotation test on the sphere, for two revolutions, left to right and back (1920 time steps) on a  $0.75^\circ$  mesh.

mesh	steps	FCR time(sec)	Mass-OBR time(sec)	ratio	FCR $L_1$ error	rate	Mass-OBR $L_1$ error	rate
$3^\circ$	480	17.4	18.2	1.0	3.25e-2	—	2.79e-2	—
$1.5^\circ$	960	132.5	151.6	1.1	1.99e-2	0.78	1.36e-3	1.04
$0.75^\circ$	1920	1184.5	1379.0	1.2	1.10e-2	0.78	5.41e-3	1.18

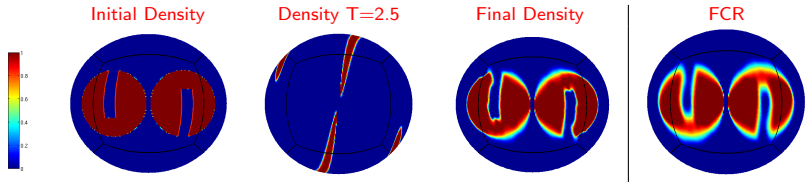
# Deformational Flow Test

For a more challenging test case we transport two notched cylinders initially centered at  $(\lambda_1, \theta_1) = (5\pi/6, 0)$  and  $(\lambda_2, \theta_2) = (7\pi/6, 0)$  in the following deformational velocity field

$$u(\lambda, \theta, t) = 2 \sin^2 \lambda \sin 2\theta \cos(\pi t/T)$$

$$v(\lambda, \theta, t) = 2 \sin(2\lambda) \cos(\theta) \cos(\pi t/T)$$

with period  $T = 5$ . In this case an adaptable target is used with parameters  $\gamma_1 = 0.1$  and  $\gamma_2 = 0.5$ , resulting in a sharper final density distribution and higher convergence rate than transport with Flux-Corrected Remap (FCR).



MVMT-a transport results for the deformational flow test on the sphere, shown at the time of maximum deformation ( $t = 2.5$ ) and at the final time ( $t = 5$ ) for a total of 2400 time steps on a mesh with  $120 \times 120$  elements per panel. FCR results shown at right.

Elements per panel	# steps	FCR time(sec)	MVMT-a time(sec)	FCR $L_1$ error	rate	MVMT-a $L_1$ error	rate
$30 \times 30$	600	45.9	46.3	$5.59e-1$	—	$4.58e-1$	—
$60 \times 60$	1200	281.3	286.9	$3.67e-1$	<b>0.61</b>	$2.49e-1$	<b>0.88</b>
$120 \times 120$	2400	2103.7	2140.3	$2.19e-1$	<b>0.68</b>	$1.25e-1$	<b>0.94</b>

Comparison of  $L_1$  errors with respect to the initial condition for Flux-Corrected Remap (FCR) and MVMT-a and comparison of computational costs as measured by Matlab<sup>TM</sup> wall-clock times in seconds, on a single Intel Xeon X5450 3.0GHz processor.

# Passive Tracer Transport

The problem:

$$\frac{\partial \rho T}{\partial t} + \nabla \cdot \rho T \mathbf{v} = 0 \quad \text{on } \Omega \times [0, T], \quad T(\mathbf{x}, 0) = T_0(\mathbf{x})$$

- Linear tracer reconstruction  $T^h(\mathbf{x})|_{c_i} = T_i + \mathbf{g}_i \cdot (\mathbf{x} - \mathbf{c}_i)$ 
  - Approximate gradient  $\mathbf{g}_i \approx \nabla T$
  - Cell center of mass  $\mathbf{c}_i = \int_{c_i} \mathbf{x} \rho^h(\mathbf{x}) dV / \int_{c_i} \rho^h(\mathbf{x}) dV$
- Target tracer  $T_i^T = \frac{\int_{\tilde{c}_i} \rho^h(\mathbf{x}) T^h(\mathbf{x}) dV}{\int_{\tilde{c}_i} \rho^h(\mathbf{x}) dV}$

## Optimization

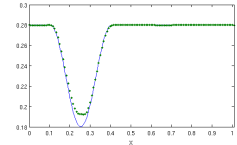
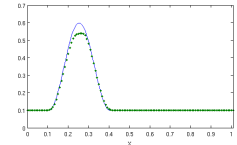
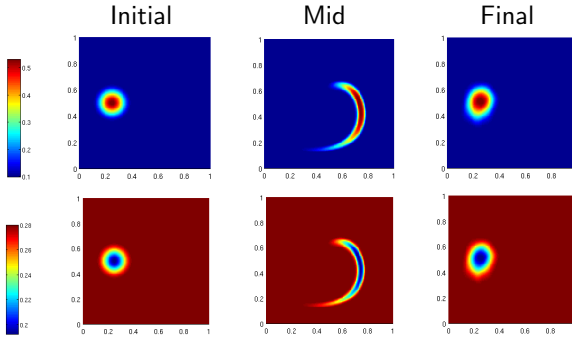
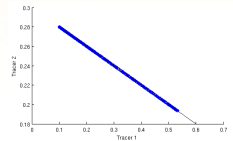
$$\left\{ \begin{array}{l} \text{minimize } \frac{1}{2} \|\tilde{T} - T^T\|_{\ell_2}^2 \quad \text{subject to} \\ \sum_{i=1}^C \tilde{m}_i \tilde{T}_i = Q \quad \text{and} \quad T_i^{\min} \leq \tilde{T}_i \leq T_i^{\max} \quad i = 1, \dots, C. \end{array} \right.$$

Challenges:

- need to solve for hundreds and even thousands of tracers simultaneously
- the tracers can be correlated, e.g.,  $\alpha T_1 + \beta T_2 = 0$

# Passive Tracer Transport

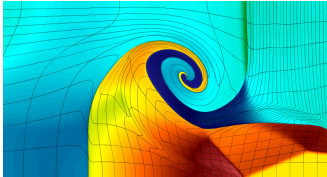
- 2 linearly correlated tracers  $T_1$  and  $T_2$
- Initial density  $\rho$  same as tracer 1
- **Linear correlation preserved under deformation!**



# High-order remap

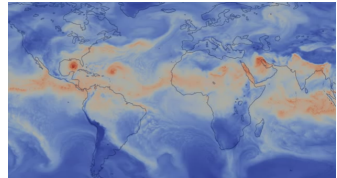
Software: **C**onstrained **O**ptimization **B**ased **R**emap **A**lgorithms

## BLAST



- Next-gen LLNL hydrocode.
- Mass-form OBR to enable conservative and (essentially) non-oscillatory high-order ALE.
- Integration of the COBRA library is in progress.
- Tzanio Kolev, et al.; LDRD.
- **Research:** Energy constraints.

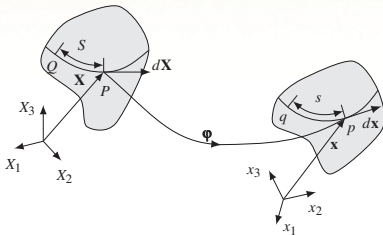
## HOMME



- The default dynamical core of the Community Atmosphere / Earth System Models.
- OBR to enable a very fast conservative and monotone semi-Lagrangian scheme.
- Mark Taylor, et al.; SciDAC 3.
- **Research:** Tracer transport.

# Tensor remap

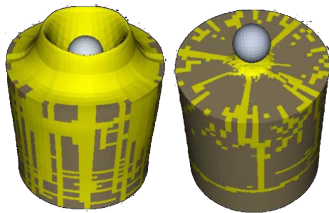
## ALEGRA



- Shock and multiphysics family of codes, including solid kinematics.
- **Challenge:** Solid kinematics schemes fail in presence of large deformations.
- **Cause:** Violation of physical constraints.
- **Deformation gradient:**  $\mathbf{F} = \frac{\partial x_i}{\partial X_A} \mathbf{e}_i \otimes \mathbf{E}_A$ .
- **Constraints — sparse but global:**

$$\text{curl } \mathbf{F}^{-1} = \mathbf{0} \quad \text{and} \quad \det \mathbf{F} > 0.$$

- Integrated interior-point methods from our Rapid Optimization Library into ALEGRA.
- Jim Kamm, Ed Love, et al.; ASC CSAR.
- **Much, much harder than scalar remap!**



# Summary

- Preservation of qualitative properties through "direct" approaches relies on the mesh, the variable placement and local "worst-case scenarios"  
⇒ imposes restrictions on mesh and/or accuracy
- Optimization-based strategies present an attractive alternative:
  - Accuracy is separated from the preservation of physical properties.
  - Physical properties can be treated as optimization constraints.
  - Discretization is relieved from securing these properties.
  - Solution is a globally optimal state: the best possible, with respect to the target state satisfying the constraints.
- OBR is more robust and accurate than explicit limiter-based remappers.
- The mass-form OBR algorithm is as fast as a local scheme.
- The optimization approach allows for specially tuned targets.
- Dual optimization variables may be used to tune targets.
- Multi-tracer transport can be done efficiently.

We've just scratched the surface - for instance, tensor remap (remap for solid deformation) needs "real" optimization.

# Publications

- P. Bochev, D. Ridzal, K. Peterson, *Optimization-based remap and transport: A divide and conquer strategy for feature-preserving discretizations*, **J. Comput. Phys.**, In Press, 2013.
- J. R. Kamm, E. Love, A. C. Robinson, J. Young, D. Ridzal, *Edge Remap for Solids*, SAND report, Sandia National Laboratories, 2013.
- K. Peterson, P. Bochev, D. Ridzal, *Optimization-based conservative transport on the cubed-sphere grid*, in Proceedings of the 9th International Conference on Large-Scale Scientific Computations, Sozopol, Bulgaria (2013).
- P. Bochev, D. Ridzal, M. Shashkov, *Fast optimization-based conservative remap of scalar fields through aggregate mass transfer*, **J. Comput. Phys.**, 246:37–57, 2013.
- P. Bochev, D. Ridzal, G. Scovazzi, and M. Shashkov, *Constrained-optimization based data transfer: A new perspective on flux correction*, in **Flux-Corrected Transport**, edited by D. Kuzmin, R. Lohner, S. Turek, Springer-Verlag, 2012.
- P. Bochev, D. Ridzal, J. Young, *Optimization-Based Modeling with Applications to Transport. Part 1. Abstract Formulation.*, In: Lirkov, I., Margenov, S., Waśniewski, J. (eds.), LSSC 2011, **LNCS**, vol. 7116, pp. 63–71. Springer, Heidelberg (2012).
- P. Bochev, J. Young, D. Ridzal, *Optimization-Based Modeling with Applications to Transport. Part 2: The Optimization Algorithm*, In: Lirkov, I., Margenov, S., Waśniewski, J. (eds.), LSSC 2011, **LNCS**, vol. 7116, pp. 72–80. Springer, Heidelberg (2012).
- D. Ridzal, P. Bochev, J. Young, K. Peterson, *Optimization-Based Modeling with Applications to Transport. Part 3: Implementation and Computational Studies*, In: Lirkov, I., Margenov, S., Waśniewski, J. (eds.), LSSC 2011, **LNCS**, vol. 7116, pp. 81–88. Springer, Heidelberg (2012).
- P. Bochev, D. Ridzal, G. Scovazzi, and M. Shashkov, *Formulation, analysis and numerical study of an optimization-based conservative interpolation (remap) of scalar fields for arbitrary Lagrangian-Eulerian methods*, **J. Comput. Phys.**, 230(13):5199–5225, 2011.